

The Nonlinear Cosmological Matter Power Spectrum with Massive Neutrinos I: The Halo Model

Kevork Abazajian¹, Eric R. Switzer², Scott Dodelson^{3,4}, Katrin Heitmann⁵ and Salman Habib¹

¹*MS B285, Theoretical Division, The University of California,
 Los Alamos National Laboratory, Los Alamos, NM 87545*

²*Department of Physics, Princeton University, Princeton, NJ 08544*

³*NASA/Fermilab Astrophysics Center Fermi National Accelerator Laboratory, Batavia, IL 60510*

⁴*Department of Astronomy & Astrophysics, The University of Chicago, Chicago, IL 60637 and*

⁵*MS D466, ISR-1, ISR Division, The University of California,
 Los Alamos National Laboratory, Los Alamos, NM 87545*

(Dated: July 30, 2018)

Measurements of the linear power spectrum of galaxies have placed tight constraints on neutrino masses. We extend the framework of the halo model of cosmological nonlinear matter clustering to include the effect of massive neutrino infall into cold dark matter (CDM) halos. The magnitude of the effect of neutrino clustering for three degenerate mass neutrinos with $m_{\nu_i} = 0.9 \text{ eV}$ is of order $\sim 1\%$, within the potential sensitivity of upcoming weak lensing surveys. In order to use these measurements to further constrain—or eventually detect—neutrino masses, accurate theoretical predictions of the nonlinear power spectrum in the presence of massive neutrinos will be needed, likely only possible through high-resolution multiple particle (neutrino, CDM and baryon) simulations.

PACS numbers: 98.80.-k, 98.65.-r, 14.60.Pq

I. INTRODUCTION

The detection of neutrino flavor oscillation in conjunction with cosmological arguments has highly constrained neutrino mass eigenvalues. Solar neutrinos [1, 2] and atmospheric neutrinos [3, 4] oscillate from one flavor to another. The KamLAND reactor neutrino detector has found evidence for neutrino oscillations consistent with the inferred solar neutrino oscillation parameters [5]. The K2K long-baseline experiment has found evidence for neutrino oscillations consistent with the atmospheric results [6]. While flavor oscillation experiments constrain only the neutrino mass differences, cosmological arguments have the advantage of constraining the total mass. The present cosmological upper limits are competitive with terrestrial experiments and expected to improve substantially with time.

Massive neutrinos influence the large scale structures of the universe in a well-defined way [7] because they do not cluster, thereby reducing the amount of matter that can accrete into potential wells. The galaxy power spectrum has been measured on large scales [8, 9] leading to upper limits on the sum of neutrino mass ranging from 0.7 to 1.8 eV [10, 11, 12, 13] (depending on assumptions and data sets). Combining estimates of the linear matter power spectrum from the Lyman- α forest in the Sloan Digital Sky Survey (SDSS) with estimates of the bias of galaxies in the SDSS with galaxy-galaxy lensing, a tight limit of 0.42 eV is inferred for the 95% C.L. limit on the sum of three degenerate mass neutrinos [14]. The approximation of a linear spectrum that is valid for such large scale measurements is no longer valid on smaller scales

where matter is highly clustered. Therefore, all studies (except for Ref. [13]) use data on the largest scales.

Using small scale data in galaxy surveys requires knowing the nonlinear clustering and bias of galaxies relative to the dark matter. As we shall show, the precision of the small scale galaxy clustering data such as that from the SDSS is not high enough to warrant the inclusion of the effect of neutrino clustering in dark matter halos, though other systematic effects may be important (see Ref. [13]). However, when large weak lensing surveys – which measure the mass distribution directly – become available, it will be essential to make direct use of this information, even on the smallest scales due to the expected precision of their results [15].

The nonlinear power spectrum for the dominant clustering component, cold dark matter (CDM) itself has been best estimated by high resolution simulations by the Virgo Collaboration [16], but their work quantifies the uncertainty in their functional fits of the nonlinear power to approximately 7%. The effects of early free-streaming of neutrinos in suppressing the linear power spectrum can be incorporated into predicting the nonlinear power spectrum such as that from the fits of Refs. [16, 17]. However, one cannot naïvely expect this to characterize the full effects of massive neutrinos in the nonlinear regime.

Vale & White [18] showed that the uncertainties introduced by approximations in ray-tracing techniques and numerical convergence of pure dark matter simulations may be sufficiently reduced with expected computing resources. Similar to the effects of neutrino infall into dark matter halos probed here, White [19] and Zhan & Knox [20] showed that the effects arising due to baryonic

cooling and heating in CDM halos can alter the nonlinear matter power spectrum to significantly alter the observed weak lensing signal. Therefore, in order to effectively use the information gained in upcoming weak surveys, one has to accurately determine the nonlinear matter power spectrum for a given cosmological model, and how it is influenced by the presence of baryons as well as massive neutrinos.

In this paper, we first describe an analytic Boltzmann solution of neutrino infall into cold dark matter (CDM) halos to calculate the modification of captured neutrinos on the halos in §II. We then employ the halo model to calculate matter clustering statistics including the effects of neutrino clustering, as well as the modification of the weak lensing power spectrum while including or ignoring this effect in §III, and then sum up our conclusions in §IV. In a companion paper [21], we use multiparticle numerical simulations to quantify the effects of massive neutrino collapse into CDM halos on the nonlinear matter power spectrum.

II. CLUSTERING OF MASSIVE NEUTRINOS IN CDM HALOS

To begin, we solve an isolated problem: how neutrinos cluster in the presence of a dark matter halo. As we will see in the next section, the neutrino clustering

around halos at late times leads to changes in the nonlinear power spectrum. These changes are unique signatures of massive neutrinos and may eventually be detected. A pioneering work [22] treated the clustering of massive neutrinos around a point-like seed with the Boltzmann equation. While this seed was taken to be a cosmic string, their technique was extended to accretion of neutrinos onto a CDM halo [23]. The density profile of a CDM halo has been found on average to follow a universal profile over a wide range of mass scales, which we take to be a Navarro-Frenk-White (NFW) form [24, 25]. The structure of the inner portion of the profile is not crucial to the neutrino clustering studied here. One assumption used in Ref. [23] that simplifies the Boltzmann solution to this problem is that the NFW CDM profile is not influenced by the accretion of neutrinos; neutrinos do not act back on the CDM. (Formally, the source term in the Boltzmann equation is a pure NFW-type CDM distribution plus the neutrinos). This approximation is reasonable because the neutrino mass associated with a cluster is a small fraction of the mass in the cluster (of order 1%, see below) and more diffusely distributed, so that changes to the CDM NFW halo are essentially negligible.

In the notation of Ref. [22], the Boltzmann solution for the Fourier transform of the neutrino profile in an evolving CDM halo is:

$$\tilde{\rho}_\nu(k, \vartheta_i, \vartheta_f) = \frac{4Gm_\nu^2 T_{\nu,0}^2 (1+z)^3}{\pi k a^3(\vartheta_f)} \int_{\vartheta_i}^{\vartheta_f} d\vartheta' a^4(\vartheta') (\tilde{\rho}_{\text{CDM}}(k, \vartheta', M_{\text{CDM}}(\vartheta')) + \tilde{\rho}_\nu(k, \vartheta_i, \vartheta')) I\left(\frac{k(\vartheta_f - \vartheta')T_{\nu,0}}{m_\nu}\right), \quad (2.1)$$

where a is the scale factor, but we parameterize integrals by a lookback super-conformal time, $d\vartheta = d\eta/a = dt/a^2$; $T_{\nu,0}$ is the current neutrino temperature, 1.95K; CDM evolution is included in the term $M_{\text{CDM}}(\vartheta')$; and

$$I(\beta) \equiv \int_0^\infty dx \frac{x \sin(\beta x)}{e^x + 1}. \quad (2.2)$$

The lower and upper limits of the ϑ integration set the time when the accretion starts, ϑ_i , and when it stops, ϑ_f . The final time is chosen to be at the redshift that the power spectrum is needed. The initial time is chosen to be early enough such that an extremely high fraction of the neutrinos have velocities that cannot be captured by CDM halos, and deep enough to be beyond the galaxy distribution of upcoming weak lensing surveys, at $z = 5$. Our results are essentially unchanged by choosing an initial $z = 3$.

Before writing down the solution for the neutrino profile, we need to add one ingredient to the earlier work [22, 23]. We will be especially interested in the features of the power spectrum and its suppression around

$k = 0.5h^{-1} \text{Mpc}$, near the transition from the 1-halo to 2-halo terms in the halo model (see below). Around $k = 0.5h^{-1} \text{Mpc}$, halos at and above $10^{14}h^{-1}M_\odot$ dominate the power spectrum [26]. These massive halos have collapsed only recently and were significantly growing during the accretion evolution history of the neutrinos. To include this, we need to insert a growth factor in the source term of the Boltzmann equation. The merging and growth of CDM clusters was studied extensively in Ref. [27], who found that they evolve as:

$$M_{\text{CDM}}(z) = M_{\text{CDM, today}} e^{-2a_c z}, \quad (2.3)$$

where the free parameter that defines the growth (a_c) is given by the phenomenological relation $M_*(a_c) = 0.018M_{\text{CDM, today}}$ [27], where M_* is the characteristic nonlinear mass, defined where the fluctuation scale $\mu(m, z) = 1$ (see below). That is, a_c is the scale factor at which a halo of mass $0.018M_{\text{CDM, today}}$ has collapsed. For very large k , on the other hand, very light clusters dominate the power spectrum and these clusters have collapsed in the distant past, so change very little during

the period from $z = 1$ until today, when most neutrino accretion takes place [23]. For increasingly large scales, the evolution of the CDM is significant: at the level of 2%, 6%, 15%, 26% for 10^{12} , 10^{13} , 10^{14} , 10^{15} solar mass halos, respectively.

As it stands, the equation for the neutrino density transform (2.1) cannot be simply integrated because the integral contains $\tilde{\rho}_\nu$. This term in the integral equation represents the clustered neutrinos acting back on themselves: as more neutrinos accrete onto a cluster, the cluster mass increases, and with it the ability to accrete more neutrinos. Since neutrinos make up a small fraction of the mass in a cluster, the effect of neutrinos pulling in more neutrinos can also be ignored as a second-order effect.

For cosmologies with more massive neutrinos that can make up a significant part of the cluster mass, the nonlinear effects of the neutrinos acting back on themselves and on the NFW-type CDM cluster may become important. Ringwald & Wong [28] found that the effect of this neutrino gravitational feedback is significant and the linearized Boltzmann equation approach underestimates neutrino infall by a small amount for less massive halos, but up to a factor of several for $\sim 10^{15} M_\odot$ halos, which are however rare. The magnitude of the effect as estimated here is therefore a minimum estimate of neutrino infall. The magnitude of the effect of infall will be quantified in detail beyond such 1-halo approaches in the multiple particle simulations in Ref. [21].

The inner $I(\beta)$ is sometimes approximated by letting the Fermi-Dirac denominator become a Boltzmann exponential [22]; then the integral can be performed analytically. But Ref. [23] points out that this approximation is off by $\approx 20\%$ for large k , so we use the full Fermi-Dirac type distribution.

The neutrino profile around a $10^{14} h^{-1} M_\odot$ halo is shown in Fig. 1. We see that neutrinos do not cluster in the halos as efficiently as cold dark matter, so the profile inwards of 100 kpc is mostly flat and saturated (recall that the dark matter NFW profile increases as r^{-1} towards the center). The CDM profile is truncated at one virial radius. The choice to cut off the CDM at its virial radius suppresses the resultant neutrino population around 1 Mpc from the halo's center.

III. THE HALO MODEL

Here we show how to include the effects of massive neutrinos within the halo model of nonlinear matter clustering and then estimate their magnitude. The halo model posits that all matter exists in halos and the correlations in the matter can be explained by considering the correlations of the halos and the density profile of matter within the halos. In the context of this model, there are two places where neutrino masses affect the total mass distribution. First, the linear power spectrum in a model with massive neutrinos differs from one with massless

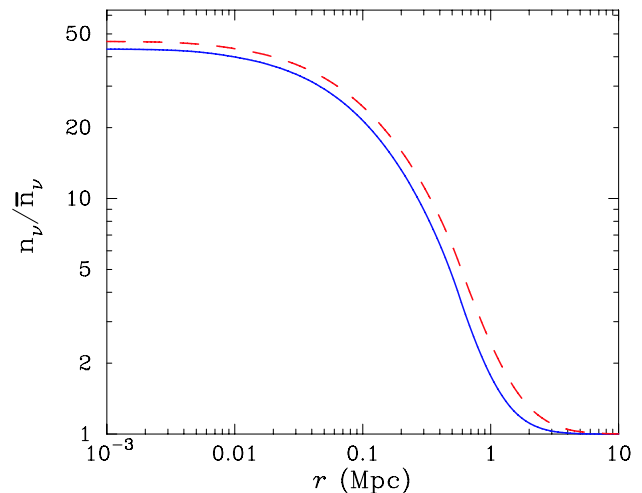


FIG. 1: A comparison of the spatial distribution of accreted neutrinos for an NFW CDM profile for a $10^{14} h^{-1} M_\odot$ halo that has evolved in the fit of Ref. [27] (solid line) and with a static profile (dashed line). The virial radius for this halo is 4.8 Mpc for a an $h = 0.7$, $\Omega_c = 0.26$ cosmology.

neutrinos. The linear power spectrum determines how halos are correlated with each other. This first effect then is felt in the power spectrum in the so-called *two-halo* term, the contribution of halo-halo correlations to the total power spectrum. This first effect is due to the free-streaming of neutrinos on large scales, in the linear regime. After CDM halos form at redshift $z \lesssim 5$, massive neutrinos do not cluster as efficiently as cold dark matter (again because of their velocities), but do fall into the potential wells of CDM halos. This second effect alters the profile of the matter within a given halo.

A. Overview

Let us first review the halo model [26, 29, 30]. (See Ref. [31] for a recent review.) The nonlinear power spectrum gets contributions from one- and two-halo terms: $P_{\text{NL}}(k) = P_{1h}(k) + P_{2h}(k)$; we first write them down and then explain the functions needed to compute them:

$$P_{2h}(k) = P_{\text{lin}}(k) \left(\int d\mu \frac{f(\mu)b(\mu)\bar{\rho}(k,\mu)}{M(\mu)} \right)^2, \quad (3.1)$$

and

$$P_{1h}(k) = \int d\mu \frac{f(\mu)}{\bar{\rho}M(\mu)} |\bar{\rho}(k,\mu)|^2. \quad (3.2)$$

Here $\bar{\rho} = \rho_{\text{crit}}\Omega_c$ is the average matter density in collapsed halos the universe, i.e. Ω_c is the fraction of the critical density that is in halos, including neutrinos that have fallen into halos. Note this is different from the usual halo model definition of $\bar{\rho}$ as the total average mass

density $\rho_{\text{crit}}\Omega_m$, where neutrinos are either not massive or ignored, and $\Omega_m = \Omega_{\text{CDM}} + \Omega_b$. Instead, we use $\Omega_c \equiv \Omega_{\text{CDM}} + \Omega_b + \Omega_{\nu\text{halo}}$. $\Omega_{\nu\text{halo}}$ is calculated by integrating the mass of neutrinos in individual halos over the halo mass function.

The halo model integrates over regions with overdensities parameterized by¹ $\mu \equiv \delta_c^2/\sigma(M)^2$, with $\delta_c = 1.68$ the linear overdensity at the epoch of a halo's collapse. Here we neglect the effects of neutrino clustering on the definition of δ_c . The rms of the linear fluctuations, $\sigma(M)$, filtered on a scale which on average contains mass M is

$$\sigma^2(M) = \int \frac{d^3k}{(2\pi)^3} P_{\text{lin}}(k) |\tilde{W}_R(k)|^2, \quad (3.3)$$

where $\tilde{W}_R(k)$ is the Fourier transform of a top-hat window function of size R , the radius enclosing mass M . Each mass M then is associated with a particular value of μ . Rare overdensities with large μ (high- σ peaks) correspond to large mass halos. The correspondence can be inverted to obtain $M(\mu)$, needed to compute the one and two-halo terms in Eqs. (3.1) and (3.2).

The number density of halos with mass M is determined solely by the dimensionless ratio μ , which quantifies how rare the overdensity is; we use the Sheth-Tormen distribution [32]

$$\frac{dn}{dM} dM = \frac{\bar{\rho}}{M} f(\mu) d\mu, \quad (3.4)$$

where

$$f(\mu) = A \frac{1}{\mu} (1 + (\alpha\mu)^{-p}) \sqrt{\alpha\mu} \exp(-\alpha\mu/2), \quad (3.5)$$

with A such that $f(\mu)$ integrated over all μ must be equal to 1 by mass conservation. We adopt $\alpha = 0.707$ and $p = 0.3$. The correlation between two halos depends on their mass. For cluster masses greater than $M(\mu = 1) \equiv M_*$, halos will be much more strongly clumped than surrounding matter. This is the nonlinear clustering regime, whose threshold is indirectly set by the linear power spectrum. The halo model bias, $b(\mu)$, folds in this mass-dependent correlation into the overall correlation of two halos, the "two halo" term. The bias associated with the Sheth-Thormen distribution is

$$b(\mu) = 1 + \frac{\mu - 1}{\delta_c} + \frac{2p}{\delta_c(1 + (\alpha\mu)^p)}. \quad (3.6)$$

B. Modification for Neutrino Clustering

The components of the halo model described above can be readily updated if neutrinos have mass. They

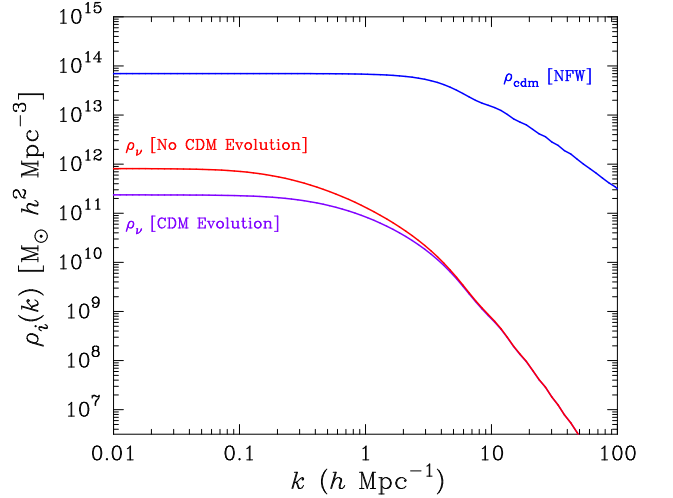


FIG. 2: A comparison of the Fourier transform of the accreted neutrino profile into an NFW CDM halo of $10^{14} h^{-1} M_\odot$ that has evolved with redshift (lower line) and with a static profile (upper line). The Fourier transform for the CDM NFW profile is shown for reference of scale.

depend solely on the linear power spectrum via σ , and one can easily insert the effect of massive neutrinos on the linear power spectrum. The final ingredient of the halo model is the mass profile around halos, represented by its Fourier transform $\tilde{\rho}(k, \mu)$ in Eqs. (3.1) and (3.2). Usually, a natural choice is the NFW form mentioned above,

$$\rho_{\text{CDM}}(r, M) = \frac{\rho_s r_s^3}{r(r + r_s)^2}. \quad (3.7)$$

Here r is the distance from the center of the halo (the conjugate variable to k), M is the halo mass, and the two parameters ρ_s and r_s are functions of M and the concentration c . In terms of these,

$$\rho_s = \frac{\Delta_v c^3(M) \bar{\rho}}{3[\ln(1 + c(M)) - \frac{c(M)}{1+c(M)}]} \quad (3.8)$$

$$r_s^3 = \frac{3M}{4\pi c(M)^3 \Delta_v \bar{\rho}}, \quad (3.9)$$

and Δ_v is the virial overdensity with respect to the mean matter density,

$$\Delta_v = \frac{18\pi^2 + 82x - 39x^2}{1 + x}, \quad (3.10)$$

and $x \equiv \Omega_c(z) - 1$ [33]. We allow the concentration to vary with redshift z and halo mass [34]

$$c(M, z) = \frac{9}{1 + z} \left(\frac{M}{M_*} \right)^{-0.13}, \quad (3.11)$$

where M_* is the cosmology-dependent characteristic nonlinear mass scale. Cluster evolution becomes nonlinear

¹ This ratio is usually denoted ν , but we use μ here to save ν for neutrinos.

for virial masses greater than M_* . The halo model is simplest if we work in Fourier space, where a given spherically symmetric density $\rho(r)$ becomes

$$\tilde{\rho}(k) = \int_0^{r_{\text{cutoff}}} (4\pi r^2 dr) \rho(r) \frac{\sin(kr)}{kr}. \quad (3.12)$$

We choose this cutoff to be at the virial radius of a given cluster $r_{\text{vir}} \equiv cr_s$.

While the NFW profile accurately describes the matter distribution if all matter is cold, it does not account for infall clustering of neutrinos. Since neutrinos have non-zero thermal velocities even at latest times, they will not strictly follow the cold dark matter profile in the halos. To account for this aspect of neutrino infall clustering, we need to generalize Eqs. 3.1 and 3.2 by letting

$$\tilde{\rho}(k, \mu) \rightarrow \tilde{\rho}_{\text{CDM}}(k, \mu) + \tilde{\rho}_\nu(k, \nu) \quad (3.13)$$

$$M(\mu) \rightarrow M_{\text{CDM}}(\mu) + M_\nu(\mu). \quad (3.14)$$

Note that, for both cold matter and for neutrinos,

$$M_i = \frac{\lim_{k \rightarrow 0} \tilde{\rho}_i(k)}{(1+z)^3}, \quad (3.15)$$

the factor of $1+z$ entering because r in Eq. (3.12) is comoving distance.

To include the effect of neutrino clustering, we add the clustered neutrino mass profile $\rho_\nu(k, \mu)$ to the halo model's k -space density. In the spherical halo model, $\rho_\nu(k, \mu)$ can be approximated by solutions to the Boltzmann equation for neutrinos around an NFW CDM halo of mass $M(\mu)$. Fig. 2 shows a comparison of the Fourier transforms of the NFW CDM halo profile and Boltzmann derived neutrino profiles. The $k \rightarrow 0$ limit of the Boltzmann Eq. (2.1) gives the total neutrino mass accreted onto a cluster, $M_\nu(\mu)$, which appears in the halo model denominators, Eqs. (3.17)-(3.18). We do not include any potential changes the the form of the mass function $f(\mu)$, since we assume the evolution of the CDM halos are unperturbed by the presence of massive neutrinos.

With these modifications, the nonlinear power spectrum becomes

$$P_{\text{NL}}^{\text{CDM}+\nu}(k) = P_{1h}^{\text{CDM}+\nu}(k) + P_{2h}^{\text{CDM}+\nu}(k), \quad (3.16)$$

$$P_{1h}^{\text{CDM}+\nu}(k) = \int d\mu \frac{f(\mu)}{\bar{\rho}[M_{\text{CDM}}(\mu) + M_\nu(\mu)]} |\tilde{\rho}_{\text{CDM}}(k, \mu) + \tilde{\rho}_\nu(k, \mu)|^2, \quad (3.17)$$

and

$$P_{2h}^{\text{CDM}+\nu}(k) = P_{lin}^{\text{CDM}+\nu}(k) \left(\int d\mu \frac{f(\mu)b(\mu)}{M_{\text{CDM}}(\mu) + M_\nu(\mu)} [\tilde{\rho}_{\text{CDM}}(k, \mu) + \tilde{\rho}_\nu(k, \mu)] \right)^2. \quad (3.18)$$

We calculate the change in the nonlinear power spectrum due to these modifications from neutrino clustering for a Λ CDM universe with parameters $\Omega_{\text{cdm}} = 0.26 - \Omega_\nu$, $h = 0.7$, $\Omega_b = 0.04$, $n = 1$ and $\sigma_8 = 0.9$. Massive neutrino models are chosen with three degenerate mass neutrinos with $m_\nu = 0.1, 0.3, 0.6, 0.9$ eV (i.e., sum of all neutrino masses of 0.3, 0.9, 1.8, 2.7 eV), with Ω_ν chosen appropriately for these masses, while σ_8 is fixed. The modification $\delta P_{\text{NL}}(k) = (P_{\text{NL}}^\nu(k) - P_{\text{NL}}^0(k))/P_{\text{NL}}^0(k)$ is shown in Fig. 3, P_{NL}^0 excludes the effects of late neutrino clustering and P_{NL}^ν includes them. Both $P_{\text{NL}}^\nu(k)$ and $P_{\text{NL}}^0(k)$ include the linear effects of early neutrino free streaming, since we are interested in the bias imposed by ignoring the effects of neutrino infall into CDM halos. The drop in power at $k \sim 0.5h \text{ Mpc}^{-1}$ occurs as expected at the scale where the most massive clusters are contributing to the nonlinear power spectrum, and increases with increasing neutrino mass. The reduction in power is due to the smooth structure of the accreted neutrino halo relative to the CDM halo.

C. Weak Lensing Convergence Power Spectrum

Planned weak lensing surveys have the potential to measure the power spectrum very accurately. Therefore, here we calculate the deviations due to massive neutrino clustering on a weak lensing observable, namely the convergence power spectrum, C_ℓ . This quantity is effectively the projected angular matter-matter power spectrum weighted by the distribution of lensed galaxies. The signal is estimated by [35, 36, 37]

$$C_\ell = \frac{9}{16} \left(\frac{H_0}{c} \right)^4 \Omega_m^2 \int_0^{\chi_h} d\chi \left[\frac{g(\chi)}{a\chi} \right]^2 P\left(\frac{\ell}{\chi}, z\right), \quad (3.19)$$

for a universe with flat geometry, where χ is the comoving radial distance, χ_h is the distance to the horizon, $a \equiv 1/(1+z)$, and $P(k, z)$ is the nonlinear power spectrum at the appropriate redshift. The weak lensing weighting function is

$$g(\chi) = \chi \int_\chi^\infty d\chi' n(\chi') \frac{\chi' - \chi}{\chi'}, \quad (3.20)$$

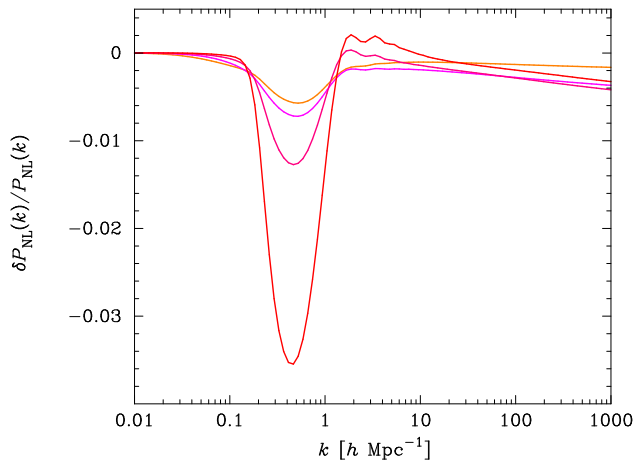


FIG. 3: The estimated change in the nonlinear matter power spectrum at $z=0$ calculated with the halo model, $\delta P_{\text{NL}}(k) = (P_{\text{NL}}^\nu(k) - P_{\text{NL}}^0(k))/P_{\text{NL}}(k)$ due to late time neutrino clustering only. (Both $P_{\text{NL}}^0(k)$ and $P_{\text{NL}}^\nu(k)$, are calculated with a transfer function that includes the same early neutrino free streaming.) The lines of increasing magnitudes denote models with three neutrinos with masses of 0.1 eV, 0.3 eV, 0.6 eV, 0.9 eV, respectively.

where $n(\chi)$ is the redshift distribution of the lensed galaxies normalized such that $\int dz n(z) = 1$.

The expected error in the observed weak lensing convergence power spectrum comes from two sources: sample variance on large scales due to finite sky coverage, and on small scales by the finite number density of galaxies on the sky,

$$\Delta C_\ell = \sqrt{\frac{2}{(2\ell+1)f_{\text{sky}}}} \left(C_\ell + \frac{\gamma_{\text{rms}}^2}{\bar{n}_{\text{gal}}} \right), \quad (3.21)$$

where the fraction of sky covered f_{sky} , intrinsic inferred galaxy ellipticity γ_{rms} , and average number density of galaxies \bar{n}_{gal} are survey dependent.

As an example, we use survey parameters similar to those possible with the Large Synoptic Survey Telescope (LSST).² Specifically, the galaxy redshift distribution is of the form $n(z) \propto z^2 e^{-(z/z_0)^2}$, with $z_0 = 1$, average galaxy density $\bar{n}_{\text{gal}} = 50 \text{ arcmin}^{-2}$, a sky coverage of $f_{\text{sky}} = 0.5$, and $\gamma_{\text{rms}} = 0.15$. In Fig. 4 we show the effect on the weak convergence power spectrum $\delta C_\ell = (C_\ell^\nu - C_\ell^0)/C_\ell^0$, when we include (C_ℓ^ν) and exclude (C_ℓ^0) the effect of neutrino clustering in CDM halos to see the dependence of the weak lensing signal. Note that the linear effect of early neutrino free streaming is included in both C_ℓ^ν and C_ℓ^0 , since we are interested in the bias imposed by ignoring the effects of neutrino infall into CDM halos. The cosmological parameters are chosen as in §III B. Here, we take the neutrino infall effect

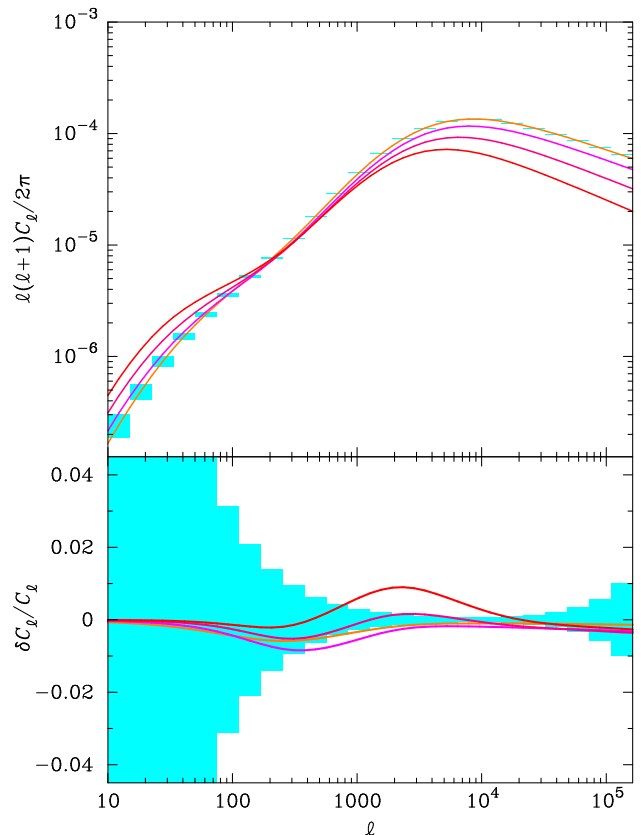


FIG. 4: The weak lensing convergence power spectrum (upper panel) for nonzero neutrino mass models of 0.1 eV, 0.3 eV, 0.6 eV, and 0.9 eV, with decreasing peak convergence, respectively. The power spectra are normalized at $\sigma_8 = 0.9$, therefore showing a pivot at $\ell \sim 200$. The deviations including and excluding this effect are plotted in the lower panel, with increasing mass neutrinos corresponding to an increased amplitude of the effect. Gray (cyan) boxes are expected errors for an LSST-like survey as described in the text.

evaluated near the peak of the weak lensing weighting function $g(\chi)$ at $z = 0.4$, causing a change in the shape of the weak convergence power spectrum deviation relative to the $z = 0$ nonlinear power spectrum above. The change in the nonlinear power spectrum affects the weak convergence power spectrum from $\sim 0.1\%$ for three 0.1 eV neutrinos to $\sim 1\%$ for three 0.9 eV neutrinos.

IV. CONCLUSIONS

We have estimated the effect of massive neutrinos in a concordance Λ CDM cosmology on the nonlinear power spectrum in the halo model. The shape of the nonlinear power spectrum is changed due to neutrino infall in CDM halos at a level of $\sim 0.5\%$ for three 0.1 eV neutrinos to $\sim 3\%$ for three 0.9 eV neutrinos, corresponding to a change in the expected shape of the weak convergence power spectrum at a level of $\sim 0.1\%$ for three 0.1 eV neutrinos

² <http://www.lsst.org/>

to $\sim 1\%$ for three 0.9 eV neutrinos, being reduced due to the weight of higher redshift structures in cosmic shear measurements.

Using the linear information from weak lensing surveys we may be able to constrain the neutrino mass so that the effect of neutrino clustering may be neglected [38]. Even given the inferred current upper limits on neutrino masses from the linear power spectrum ($\Sigma m_{\nu_i} < 0.42$ eV, 95% C.L.) [14], the effect of neutrino clustering may be negligible unless current neutrino mass upper limits from the linear power spectrum are too stringent, or new degeneracies may emerge among features in the primordial power spectrum (e.g., running of the primordial spectral index [39] or a break in the spectrum [40]) which allow for larger neutrino masses.

For more general cases where massive neutrinos are present in fits to observed weak lensing convergence power spectra, massive neutrinos will need to be included in numerical simulation predictions of the weak lensing signal in addition to phenomena arising from baryonic

condensation and heating [19, 20], leading to the potential necessity of high-resolution multiparticle (neutrino, CDM and baryon) hydrodynamic numerical simulations. Coupled with upcoming weak lensing surveys, these predictions will be a power probes of the contents of the cosmological soup as well as the process of cosmological structure formation.

Acknowledgments

We are grateful to Lam Hui, Dragan Huterer, Anatoly Klypin, Lloyd Knox, Chung-Pei Ma, Andreas Ringwald and Tony Tyson for useful discussions and comments on a draft. KA, SH, and KH are supported by Los Alamos National Laboratory (under DOE contract W-7405-ENG-36). SD is supported by Fermilab (under DOE contract DE-AC02-76CH03000) and by NASA grant NAG5-10842.

-
- [1] Super-Kamiokande, S. Fukuda *et al.*, Phys. Rev. Lett. **86**, 5656 (2001), [hep-ex/0103033].
 - [2] SNO, Q. R. Ahmad *et al.*, Phys. Rev. Lett. **89**, 011301 (2002), [nucl-ex/0204008].
 - [3] Super-Kamiokande, Y. Fukuda *et al.*, Phys. Rev. Lett. **81**, 1562 (1998), [hep-ex/9807003].
 - [4] Super-Kamiokande, S. Fukuda *et al.*, Phys. Rev. Lett. **85**, 3999 (2000), [hep-ex/0009001].
 - [5] KamLAND, K. Eguchi *et al.*, Phys. Rev. Lett. **90**, 021802 (2003), [hep-ex/0212021].
 - [6] K2K, M. H. Ahn *et al.*, Phys. Rev. Lett. **90**, 041801 (2003), [hep-ex/0212007].
 - [7] J. R. Bond and A. S. Szalay, Astrophys. J. **274**, 443 (1983).
 - [8] W. J. Percival *et al.*, Mon. Not. Roy. Astron. Soc. **327**, 1297 (2001), [astro-ph/0105252].
 - [9] SDSS, M. Tegmark *et al.*, Astrophys. J. **606**, 702 (2004), [astro-ph/0310725].
 - [10] O. Elgaroy and O. Lahav, JCAP **0304**, 004 (2003), [astro-ph/0303089].
 - [11] D. N. Spergel *et al.*, Astrophys. J. Suppl. **148**, 175 (2003).
 - [12] SDSS, M. Tegmark *et al.*, Phys. Rev. **D69**, 103501 (2004), [astro-ph/0310723].
 - [13] K. Abazajian *et al.*, astro-ph/0408003.
 - [14] U. Seljak *et al.*, astro-ph/0407372.
 - [15] A. Refregier *et al.*, Astron. J. **127**, 3102 (2004), [astro-ph/0304419].
 - [16] The Virgo Consortium, R. E. Smith *et al.*, Mon. Not. Roy. Astron. Soc. **341**, 1311 (2003), [astro-ph/0207664].
 - [17] J. A. Peacock and S. J. Dodds, MNRAS **280**, L19 (1996).
 - [18] C. Vale and M. J. White, Astrophys. J. **592**, 699 (2003), [astro-ph/0303555].
 - [19] M. J. White, astro-ph/0405593.
 - [20] H. Zhan and L. Knox, astro-ph/0409198.
 - [21] K. Heitmann *et al.*, in preparation (2004).
 - [22] R. H. Brandenberger, N. Kaiser and N. Turok, Phys. Rev. **D36**, 2242 (1987).
 - [23] S. Singh and C.-P. Ma, Phys. Rev. **D67**, 023506 (2003), [astro-ph/0208419].
 - [24] J. F. Navarro, C. S. Frenk and S. D. M. White, Astrophys. J. **462**, 563 (1996), [astro-ph/9508025].
 - [25] J. F. Navarro, C. S. Frenk and S. D. M. White, Astrophys. J. **490**, 493 (1997).
 - [26] U. Seljak, Mon. Not. Roy. Astron. Soc. **318**, 203 (2000), [astro-ph/0001493].
 - [27] R. H. Wechsler, J. S. Bullock, J. R. Primack, A. V. Kravtsov and A. Dekel, Astrophys. J. **568**, 52 (2002), [astro-ph/0108151].
 - [28] A. Ringwald and Y. Y. Y. Wong, hep-ph/0408241.
 - [29] J. A. Peacock and R. E. Smith, Mon. Not. Roy. Astron. Soc. **318**, 1144 (2000), [astro-ph/0005010].
 - [30] R. Scoccimarro, R. K. Sheth, L. Hui and B. Jain, Astrophys. J. **546**, 20 (2001), [astro-ph/0006319].
 - [31] A. Cooray and R. Sheth, Phys. Rept. **372**, 1 (2002), [astro-ph/0206508].
 - [32] R. K. Sheth and G. Tormen, Mon. Not. Roy. Astron. Soc. **308**, 119 (1999), [astro-ph/9907024].
 - [33] G. L. Bryan and M. L. Norman, Astrophys. J. **495**, 80 (1998), [astro-ph/9710107].
 - [34] J. S. Bullock *et al.*, Mon. Not. Roy. Astron. Soc. **321**, 559 (2001), [astro-ph/9908159].
 - [35] W. Hu and M. Tegmark, Astrophys. J. Lett. **514**, L65 (1999), [astro-ph/9811168].
 - [36] M. Bartelmann and P. Schneider, Phys. Rept. **340**, 291 (2000), [astro-ph/9912508].
 - [37] S. Dodelson, *Modern Cosmology* (Academic Press, San Diego, 2003).
 - [38] K. N. Abazajian and S. Dodelson, Phys. Rev. Lett. **91**, 041301 (2003), [astro-ph/0212216].
 - [39] U. Seljak *et al.*, astro-ph/0406594.
 - [40] A. Blanchard, M. Doust, M. Rowan-Robinson and S. Sarkar, Astron. Astrophys. **412**, 35 (2003), [astro-ph/0304237].